
*9th International Conference on Fibre-Reinforced Polymer (FRP) Composites in Civil Engineering (CICE 2018), PARIS 17-19 JULY 2018*

# FLEXURAL BEHAVIOUR OF AN INNOVATIVE CONNECTION FOR STRUCTURAL SANDWICH PANELS

R. Lameiras [1], J. Barros[2], I.B. Valente[2] and M. Azenha[2]
[1] *University of Brasília – UnB, Campus Darcy Ribeiro, FT-ENC, Brasília, Brazil, email: rmlameiras@unb.br*
[2] *University of Minho, Campus de Azurém, Guimarães, Portugal*

## ABSTRACT

This paper presents the results experimental work conducted with composite beam specimens that are part of a series of studies to determine the feasibility of using a new type of shear connector, called PERFOFRP, in Steel Fibre Reinforced Self-Compacting Concrete (SFRSCC) structural sandwich wall panels. The connector is consisted of a flat Glass Fiber Reinforced Polymer (GFRP) plate with aligned holes evenly distributed along its length. The perforated part of connector is embedded in the concrete layers and the connection is materialized by the combined effects of friction/adhesion and of the mechanical interlock between the perforated laminate and the concrete dowels formed by the concrete that pass through the holes. Previously, the authors of the present paper investigated the mechanical behaviour of connections made with PERFOFRP connectors under transversal loads. Nonetheless, up to now, no investigation was published on the flexural behaviour of sandwich panels produced with the PERFOFRP connectors. In the present paper, the overall mechanical behaviour of the connection under flexure was investigated, being reported: failure modes, stiffness and ultimate flexural capacities of composite beams. The impact of using connectors made with two different types of GFRP laminates were investigated on the mechanical behaviour of composite beams was investigated.

## KEYWORDS

Hybrid structures, Characterization of FRP and FRC materials/systems, Sandwich panel, Connector, PERFOFRP, Flexural behaviour.

## INTRODUCTION

Concrete structural sandwich wall panel is basically a concrete-insulation-concrete sandwich in which the outer concrete layer usually resists the external horizontal loads (i.e.; wind and mechanical impacts) and the internal concrete layer generally acts together with the external layer to resist the horizontal loads and usually also withstand eventual vertical loads due to the slabs and their use. An essential component of a concrete sandwich panel is the connection between the concrete layers. The connections must be capable to transit all the stress components between this two concrete layer, where the in-plane shear and the longitudinal stress components are those governing the design of this connector.

In the search for improved thermal efficiency of sandwich panels, different types of Fibre-Reinforced Polymer (FRP) connectors have been proposed by several researchers for reinforced/prestressed concrete sandwich panels (Einea, 1992, Salmon et al., 1997, Davies, 2001, Rizkalla et al., 2009, Benayoune et al., 2008, PCI Committee on Precast Sandwich Wall Panels, 2011, Tomlinson, 2015), and some of them are even commercially available (PCI Committee on Precast Sandwich Wall Panels, 2011, Naito et al., 2012).

In 2013, the authors of this paper proposed an innovative sandwich panel consisting on Steel Fibre Reinforced Self-Compacting Concrete (SFRSCC) outer layers connected by Glass Fibre Reinforced Polymer (GFRP) perforated plates, hereinafter referred as PERFOFRP connectors (Lameiras et al., 2013a, Lameiras et al., 2013b, Lameiras et al., 2018). The interest of this innovative connection system lies in two major aspects: first, the GFRP is a material characterized by its relatively low thermal conductivity, avoiding the thermal bridges and, consequently, increasing the thermal efficiency of the sandwich wall panel, and, secondly, the plate geometry of this connector is appropriate for its use in practice and the adoption of most effective and competitive production methods for the prefabrication of sandwich panels of better quality and lower price when compared with the traditional solutions.

This paper reports the results of experimental tests executed to assess the mechanical relative effectiveness of the connections between PERFOFRP and SFRSCC in loading conditions representative of the real application. For a better understanding of the structural behaviour of the panels, this paper centres efforts for assessing the influence of use of two types of GFRP on the ductility and strength capacity of connections under flexure.

## METHODS

Six composite small scale beam specimens subjected to a symmetrical two-point load were tested at Laboratory of the Structural Division of the University of Minho. Details about the specimens, materials and experimental procedure are provided in the following sections.

### Geometry and Materials

Each specimen consisted of a sandwich beam with length of 1245 mm, rectangular section with an overall thickness of 180 mm and width of 200 mm. Each specimen was composed of three layers with 60 mm thickness, the outer layers are made by Steel Fibre Reinforced Self-Compacting Concrete (SFRSCC), while the core layer is constituted by Expanded Polystyrene (EPS). The arrangement of the layers, their thickness and the materials were chosen to be representative of the sandwich wall panels previously optimized through parametric studies with Finite Element analyses (Lameiras et al., 2013b). The SFRSCC layers were connected with a continuous PERFOFRP connector positioned in the middle of the beam's cross section along all its length, as shown in Fig. 1.

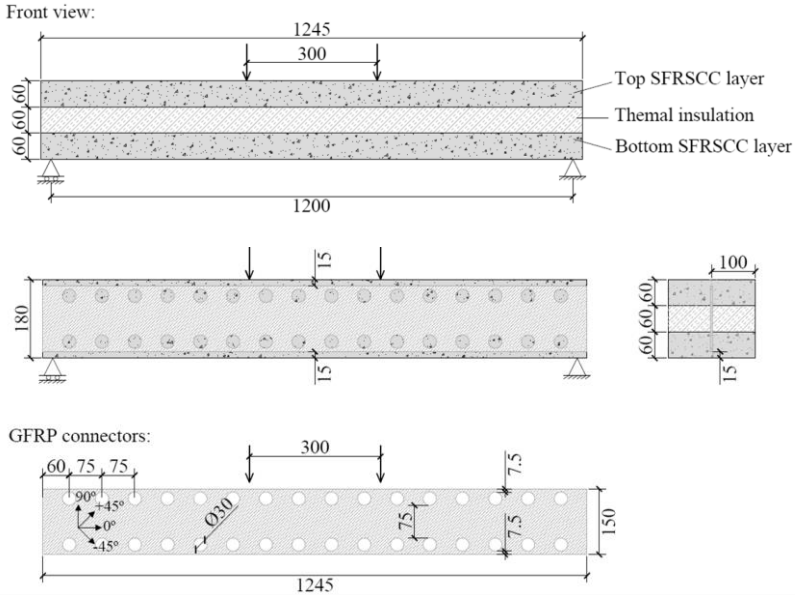


*Figure 1: Geometry of test specimen (units in millimetres).*

The PERFOFRP connector used in this work was designed to have the same hole diameter (30 mm) and spacing used in the connectors previously tested under pull-out and push-out loads (Lameiras et al., 2018). The diameter of holes (30 mm) and the SFRSCC cover thickness (15 mm) was determined for assuring the passage of the fresh SFRSCC through the holes and the gap between the connector and the formwork without the occurrence of segregation of aggregates and fibres. This thickness aims also to protect the GFRP connector, is also predicted to avoid the formation of a line on the external surfaces of the panel coinciding with the location of the connector (due to the different physical properties of GFRP and SFRSCC), since the occurrence of these lines would have negative impact on the appearance of the panel. The diameter of the holes, as well as its cover thickness of 7.5 mm have also attended the stress concentration and failures modes observed in the pull-out and push-out tests (Lameiras et al., 2018).

The SFRSCC consisted of ordinary Portland cement (413 kg/m$^3$) type CEM I 42.5 R according to EN 197-1: 2011 (European Committee for Standardization, 2011), fine river sand (233 kg/m$^3$), coarse river sand (700 kg/m$^3$), limestone filler (353 kg/m$^3$), crushed limestone coarse aggregate with 12 mm maximum size (582 kg/m$^3$), water (148 kg/m$^3$), SIKA ViscoCrete 3005 superplasticizer (7.83 kg/m$^3$) and hooked-end steel fibres (60 kg/m$^3$). The steel fibres were characterized by a length ($L_f$) equal to 35 mm, a diameter ($d_f$) equal to 0.55 mm, and an aspect ratio ($\lambda_f = L_f/d_f$) of 65. According to the data given by the supplier, their yield stress ranges between 1244 and 1446 MPa. The compressive characteristics of the SFRSCC were determined from seven 150 ×300 mm diameter × height cylinders tested after 31 days of curing. The average compressive strength ($f_{cm}$) was 45.27 MPa (CoV of 1.0%), obtained following the procedures given in EN 12390-3 (CEN, 2009). An average modulus of elasticity ($E_c$) of 34.20 GPa (CoV of 1.1%) was obtained. The flexural-tensile behaviour of SFRSCC was obtained from five notched three-point beam tests (3PBTs) performed on prisms of 150 mm square cross section and 600 mm length, following the recommendations of RILEM TC 162-TDF (RILEM TC 162-TDF, 2000) in terms of the loading and casting procedures. From the three point notched beam tests (3PBTs), the following results

were determined: limit of proportionality ($f_{fct,L}$); equivalent ($f_{eq,2}$ and $f_{eq,3}$) and residual ($f_{Ri}$, with $i$=1 to 4) flexural tensile strength parameters . The $f_{R1}$, $f_{R2}$, $f_{R3}$ and $f_{R4}$ is the flexural stress corresponding to the CMOD of 0.5, 1.5, 2.5 and 3.5 mm, respectively, as recommended by the *fib* Model Code. The average values (coefficient of variation; lower bound value determined with 95% of confidence level) obtained for $f_{fct,L}$, $f_{eq,2}$ , $f_{eq,3}$, $f_{R1}$, $f_{R2}$, $f_{R3}$, $f_{R4}$ were, respectively, 5.80 MPa (13.3%; 5.13 MPa), 9.62 MPa (12.4%; 8.57 MPa), 8.10 MPa (15.0%; 7.03 MPa), 9.21 MPa (13.8%; 8.10 MPa), 8.11 MPa (15.4%; 7.02 MPa), 6.82 MPa (15.7%; 5.88 MPa) and 4.13 MPa (19.4%; 3.22 MPa).

According to the data supplied by the manufacturer, the EPS adopted in the middle layer, as an insulating material, has an apparent density of 15 kg/m$^3$.

Two different GFRP laminates were adopted for the PERFOFRP connectors. Both were produced by Vacuum Assisted Resin Transfer Moulding (VARTM), and were made by glass fibre reinforcement and polyester resin matrix. The first laminate, hereinafter called CSM, consisted of five layers of Chopped Strand Mat (CSM) with 450 g/m$^2$ of E-glass fibres per each layer. This reinforcement is characterized by short length fibres randomly oriented in its plane. The second laminate, MU4, consisted of bi-axial Stitched Roving Fabric (SRF) and unidirectional mat, with their continuous reinforcement arranged on ±45° and 0° directions. The average final thickness of laminates was 2.0 mm for CSM and 4.0 mm for MU4 laminates. Fibre contents, by volume, equal to 41 % and 49 % were determined for CSM and MU4 composites, respectively. The tensile properties of the composites were determined from direct tensile tests performed with six specimens of each type, with the loading direction respect to fibre system orientation represented in the inset of Fig. 2, considered 0°. The direct tensile tests followed the procedures described in ASTM D3039 (ASTM, 2008). The engineering tensile stress was assumed as the ratio between the registered load and the average cross-sectional area of specimen, while the engineering axial strain was determined by attaching a clip-gauge transducer with a reference length of 50 mm to the mid-span of specimen. The ultimate tensile stress, the elastic limit stress, the corresponding strains and the tensile modulus of elasticity obtained in these tests are shown in Table 1. The stress−strain curves obtained from tension coupon tests are represented in Fig. 2. The shear properties of CSM laminate were obtained by testing four specimens in a standard Iosipescu apparatus following the procedures described in ASTM D5379 (ASTM, 2012). Average shear strength of 139.60 MPa, ultimate shear strain of 19510 με and shear modulus of 3.97 GPa were obtained with coefficient of variation of 1.2 %, 16.4 % and 2.5 %, respectively.

Table 1: Relevant results obtained from the direct tensile tests with CSM and MU4 specimens.

| FRP | Dir. | Ultimate tensile stress $\sigma_{pt.u}$ | | Ultimate tensile strain $\varepsilon_{pt.u}$ | | Elastic limit stress $\sigma_{pt.el}$ | | Elastic limit strain $\varepsilon_{pt.el}$ | | Tensile modulus of elasticity $E_{pt}$ | |
|---|---|---|---|---|---|---|---|---|---|---|---|
| | | Avg. [MPa] | CoV | Avg. [με] | CoV | Avg. [MPa] | CoV | Avg. [με] | CoV | Avg. [GPa] | CoV |
| CSM | - | 252.54 | 8.5% | 18029 | 9.8% | 252.54 | 8.5% | 18029 | 9.8% | 14.64 | 7.4% |
| MU4 | 0°/90° | 183.48 | 8.5% | 26788 | 2.3% | 73.44 | 4.3% | 5016 | 3.8% | 16.70 | 3.0% |

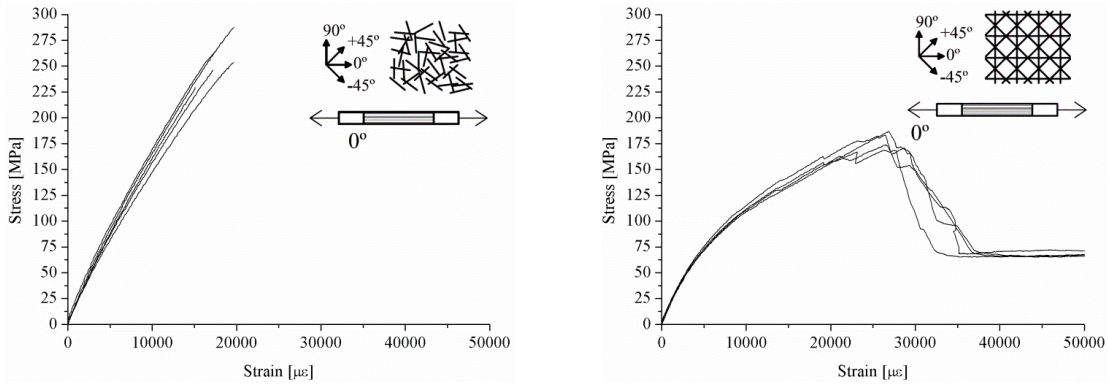


(a) CSM (b) MU4

*Figure 2: Stress versus strain response obtained in direct tensile tests with specimens representative of PERFOFRP connectors made by different laminates.*

Three identical sandwich beams were cast for each type of GFRP used in the PERFOFRP connectors. Initially, the connector was positioned in the middle of each beam. The bottom SFRSCC layer was poured up to the 60 mm level marked in the wood form. Two EPS blocks with the same length of the beam and 60 mm of thickness were positioned in each side of GFRP connector. The top SFRSCC layer was then poured. All the specimens were covered with plastic foil, and twenty four hours after the casting procedure they were removed from mold to cure in air until testing. The tests were conducted when the specimens attained an age between 114 and 120 days.

**Test setup, instrumentation and test procedure**

The beam specimens were tested under the four-point bending loading configuration represented in Fig. 3. The load was applied by a 500 kN hydraulic jack via a load-spreader I-section steel beam and two halves of steel cylinders that were in contact to the top surface along all the width of the beam's cross section. The beams were simply-supported on steel rollers, with a span of 1200 mm. One of the supports had the rotation and sliding released in the direction parallel to the specimen's axis. All the specimens were tested with the beams positioned in the same direction that they were casted, that is, with their rough surface of the top SFRSCC layer upside.

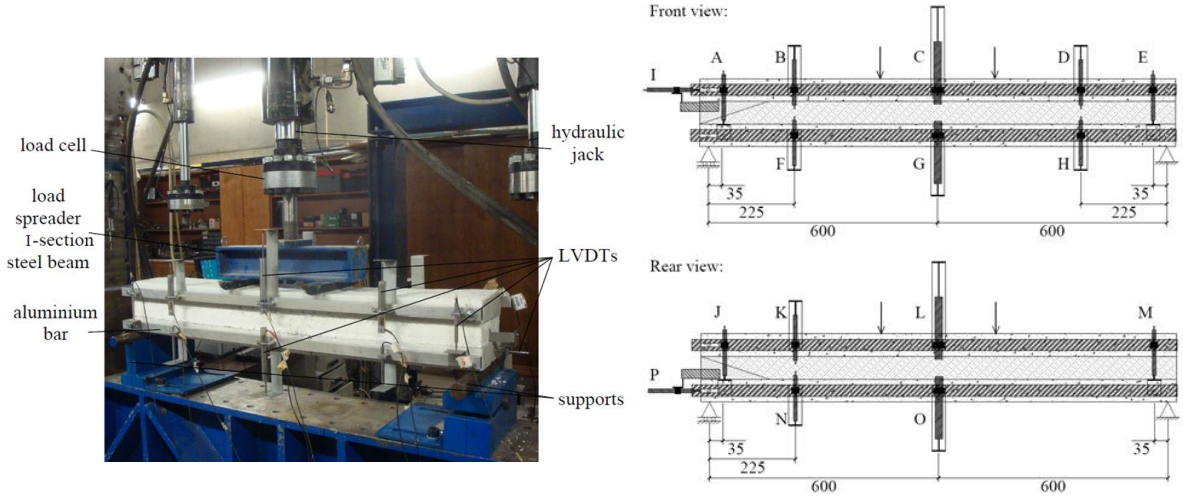


*Figure 3: Test setup and instrumentation (units in millimetres).*

The load was registered by a 250 kN capacity load cell attached at the extremity of the hydraulic jack (see Fig. 3). The following monitoring system was installed: (1) Ten LVDTs for measuring deflections along the beam's span (LVDTs C, G, L and O, with a stroke of ±50 mm) and at a distance of 225 mm from the supports (B, D, F, H, K and N, with stroke of ±25 mm). To evaluate possible misalignment of loading application, in the first and second specimens of each series, deflections were obtained in the front and rear sides of beams, as shown in Fig. 3. In the third specimen of each series deflections were obtained only in the rear side of beam. Deflections were obtained from measurements in the LVDTs fixed to an auxiliary steel bar in order do not include parasitic displacements in measurements (Japan Society of Civil Engineers, 1984). The measurements of deflections of top and bottom SFRSCC layers were made independently; (2) Two LVDTs (stroke of ±10 mm) were used to measure the end slips (longitudinal direction) between the PERFOFRP and the SFRSCC layers (LVDTs I and P). (3) Four LVDTs (stroke of ±2.5 mm) were used to measure the relative displacement (i.e.; transversal direction) between the top and bottom SFRSCC layers (LVDTs A, E, J and M). The arrangement of LVDTs is shown in Fig. 3.
A hundred unloading-reloading cycles between 0 to 14 kN were applied at the beginning of testing the third specimen of each series. During the load cycles, the test was load controlled at 1.02 kN/s, and afterwards the test was controlled by deformation at 0.005 mm/s. The loading was conducted until the specimen's load carrying capacity drops at least 50% of its maximum capacity. All measurements made by the load cell and LVDTs were registered continuously along all the test at a rate of 2 Hz.

**RESULTS AND DISCUSSIONS**

The experimentally obtained cracking load, maximum applied load and maximum midspan deflection for each specimen are summarized in Table 2. The load-deflection curves are shown in Fig. 4.
Table 2: Cracking load, maximum applied load and midspan deflection corresponding to the maximum applied load.

| Specimen Ref. | Cracking load | | | Maximum applied load | | | Midspan deflection corresponding to the maximum applied load | | |
|---|---|---|---|---|---|---|---|---|---|
| | Value [kN] | Avg | CoV [%] | Value [kN] | Avg | CoV [%] | Value [mm] | Avg | CoV [%] |
| CSM 01 | 15.5 | | | 25.4 | | | 1.62 | | |
| CSM 02 | 14.3 | 14.7 | 5 | 28.3 | 26.1 | 7 | 1.77 | 1.6 | 12 |
| CSM 03 | 14.2 | | | 24.7 | | | 1.40 | | |
| MU4 01 | 15.7 | | | 32.2 | | | 17.33 | | |
| MU4 01 | 15.6 | 15.6 | 1 | 27.9 | 29.6 | 8 | 17.01 | 16.2 | 11 |
| MU4 03 | 15.5 | | | 28.8 | | | 14.11 | | |

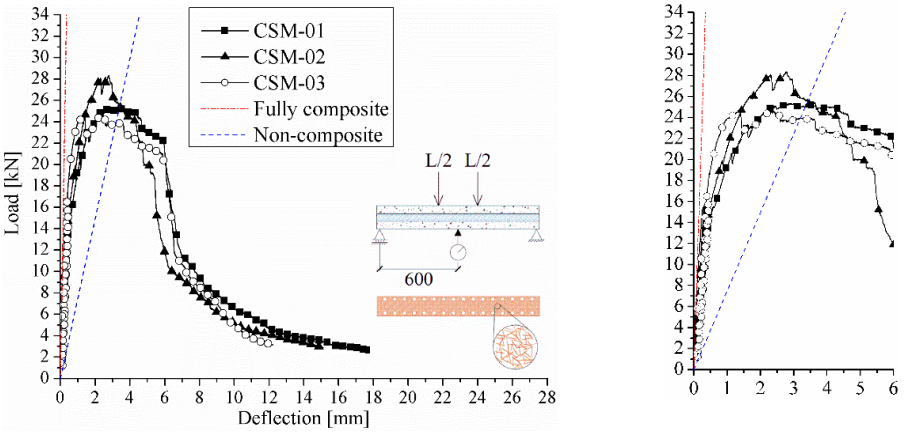


*(a) CSM*

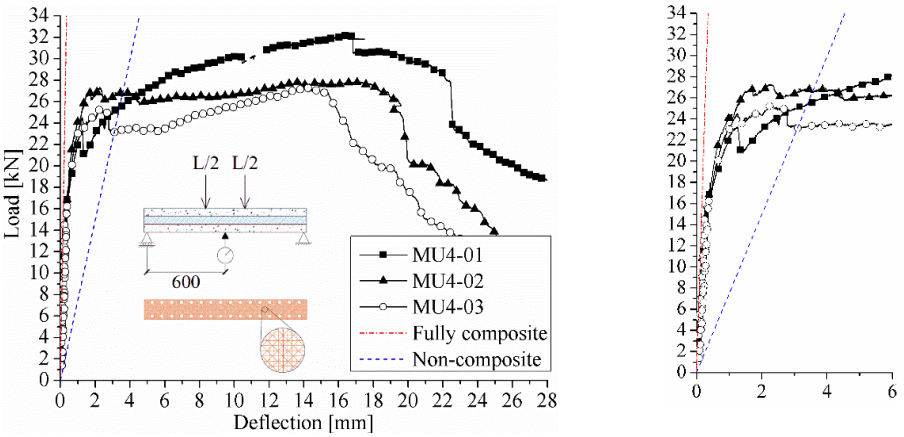


*(b) MU4*

*Figure 4: Average load-midspan deflection curves for CSM and MU4 specimens.*

The deflections calculated for the upper concrete layer were obtained as the measured deflection diminished by the average vertical displacement recorded in the support ends (recorded in the LVDTs A, E, J and M).

All the specimens of each group presented similar experimental responses. In general, the responses are characterized by an initial linear branch until the occurrence of the first crack, after which the initial stiffness of the specimen has decreased. Flexural cracks were first observed at the bottom and front sides of the bottom SFRSCC layer. The average cracking load was 14.7 kN (st. dev. equal to 0.74 kN) and 15.6 kN (st. dev. equal to 0.16 kN) for specimens made with CSM and MU4 laminates, respectively. These cracks progressed transversely across the underside of the bottom SFRSCC layer, and were located in the "pure" bending zone. Other hairline cracks occurred in the bottom SFRSCC layer within the flexure/shear spans.

At this stage, for CSM specimens, these cracks propagated progressively towards the top of the bottom SFRSCC of sandwich panel. Then, some hairline cracks also appeared in the bottom face of the top SFRSCC layer. The CSM specimens attained an average maximum load of 26.08 kN. For a deflection just after the one corresponding to the peak load a louder sound was heard, and the width of one of the cracks that appeared in the bottom SFRSCC layer started to increase, while the other cracks almost cease to propagate. Then, the load was decreasing pronouncedly with the increase of the deflection.

For the MU4 specimens, after the cracks in the top SFRSCC layer have formed, a longitudinal crack appeared in the upper surface of the top SFRSCC layer, aligned with the PERFOFRP connector. Subsequently, this longitudinal crack extended over the length of the beam, and the crack opening has increased. Thereafter, new cracks opened in the top SFRSCC layer, and similar to what occurred for the CSM specimen, a louder sound was heard, and one of the cracks of the bottom SFRSCC layer degenerated in a macro-crack. A more intense cracking and wider cracks were also noticed for the specimens made with MU4 connector. The failure of these specimens occurred after a sequence of louder noises, typical of the failure of the GFRP laminates under direct tension. At this stage the load-carrying capacity of sandwich beam dropped suddenly.

After the tests, the specimens were disassembled in order to analyze the anchorage conditions of the connectors. The final aspect of some connectors are shown in Fig. 5. After the observation of the final aspect of connectors, the failure of the sandwich beams was therefore attributed to the rupture of the GFRP connectors caused by the propagation of flexural cracks. Similarly to the behaviour of the composites under direct tensile tests (see Fig. 2), the specimen made with CSM connectors presented a more brittle behaviour when compared to the behaviour of specimens with MU4 laminates. Moreover, the first sound heard during the tests was probably related to the failure of the laminates in the region right below the holes. After this rupture the neutral axes of the beam's cross section in this region naturally was shifted upward. In the case of MU4 connectors, a new equilibrium was attained because the tensile strength of the laminate, together with the post-cracking residual strength of the SFRSCC, were able to carry the higher load transferred to the connector. Nonetheless, for the specimens made with CSM connectors, the smaller ductility of this type of connector conducted to a more abrupt load decay of the beam just after damage initiation in the connector. Fig. 5 evidences that a "discrete crack" was formed in the CSM connector (localized failure), while a damage zone was developed in the MU4 connector (smeared damage).

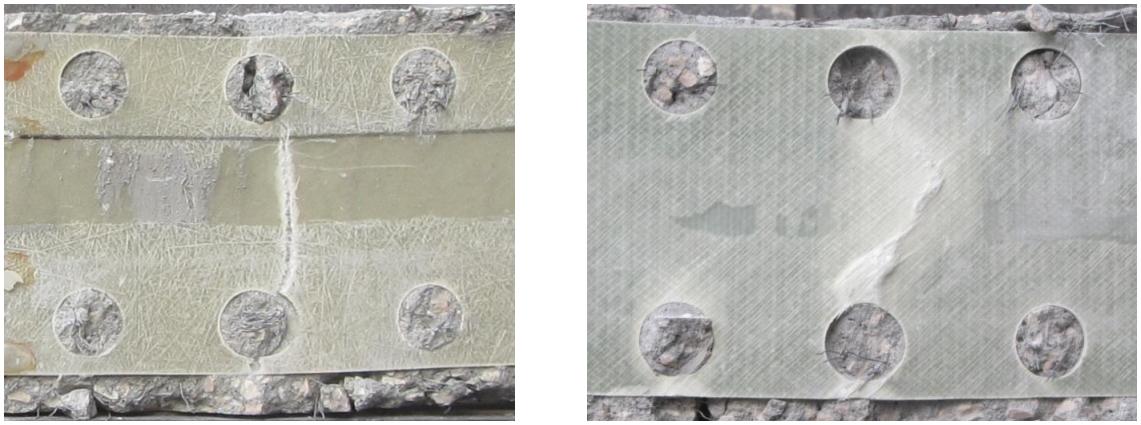

(a) CSM-02 (b) MU4-01

Figure 5: Final aspect of connectors after failure of sandwich beams.

## CONCLUSIONS

This paper performed an experimental investigation on the flexural behaviour of connections for sandwich panels containing PERFOFRP connectors and SFRSCC layers. Sandwich beams made with two different types of GFRP connectors (i.e.; CSM and MU4) were tested under four-point bending, and the results were analyzed in terms of deflections and failure mechanisms. The main conclusions derived from the experimental investigations are the following ones:

- Independently on the type of laminate used in the connector, the ultimate failure mechanism of the connections under flexure is always associated to the flexural failure of the PERFOFRP connector after an extensive cracking in the SFRSCC layers.
- Although no significant increase on the cracking or ultimate load of the tested sandwich beams were obtained by replacing CSM connector by another stiffer connector, MU4, the failure mode obtained in the beams made with MU4 laminates was much more ductile.

**ACKNOWLEDGMENTS**

Authors would like to thank the companies Mota-Engil, Civitest and PIEP. The authors also thank the collaboration of the following companies: Maccaferri for supplying the fibres and BASF for providing the superplasticizer.

**REFERENCES**

ASTM 2008. D3039 / D3039M: Tensile properties of polymer matrix composite materials. West Conshohocken, PA: ASTM International.

ASTM 2012. D5379 - 12: Test method for shear properties of composite materials by the V-notched beam method. West Conshohocken, PA: American Society for Testing and Materials (ASTM).

BENAYOUNE, A., SAMAD, A. A. A., TRIKHA, D. N., ALI, A. A. A. & ELLINNA, S. H. M. 2008. Flexural behaviour of pre-cast concrete sandwich composite panel – Experimental and theoretical investigations. *Journal of Construction and Building Materials,* 22**,** 580-592.

CEN 2009. EN 12390-3. Testing hardened concrete – Part 3: compressive strength of specimens. Lisbon: European Committee for Standardization (CEN).

DAVIES, J. 2001. *Lightweight sandwich construction*, Wiley-Blackwell.

EINEA, A. 1992. *Structural and thermal efficiency of precast concrete sandwich panel systems.* Ph.D, University of Nebraska.

EUROPEAN COMMITTEE FOR STANDARDIZATION 2011. EN 197-1: Cement. Composition, specifications and conformity criteria for common cements.

JAPAN SOCIETY OF CIVIL ENGINEERS 1984. JSCE-SF4: Method of tests for flexural strength and flexural toughness of steel fiber reinforced concrete. Part III-2 Method of tests for steel fiber reinforced concrete. Concrete library of JSCE.

LAMEIRAS, R., BARROS, J., AZENHA, M. & VALENTE, I. B. 2013a. Development of sandwich panels combining fibre reinforced concrete layers and fibre reinforced polymer connectors. Part I: conception and pull-out tests. *Composite Structures,* 105**,** 446-459.

LAMEIRAS, R., BARROS, J., AZENHA, M. & VALENTE, I. B. 2013b. Development of sandwich panels combining fibre reinforced concrete layers and fibre reinforced polymer connectors. Part II: Evaluation of mechanical behaviour. *Composite Structures,* 105**,** 460-470.

LAMEIRAS, R., VALENTE, I. B., BARROS, J. A. O., AZENHA, M. & GONÇALVES, C. 2018. Pull-out behaviour of Glass-Fibre Reinforced Polymer perforated plate connectors embedded in concrete. Part I: Experimental program. *Construction and Building Materials,* 162**,** 155-169.

NAITO, C., HOEMANN, J., BEACRAFT, M. & BEWICK, B. 2012. Performance and Characterization of Shear Ties for Use in Insulated Precast Concrete Sandwich Wall Panels. *Journal of Structural Engineering,* 138**,** 52-61.

PCI COMMITTEE ON PRECAST SANDWICH WALL PANELS 2011. State-of-the-art of Precast/Prestressed Sandwich Wall Panels. *Precast/Prestressed Concrete Institute Journal,* 56**,** 131-175.

RILEM TC 162-TDF 2000. Bending test. *Materials and Structures,* 33**,** 3-5.

RIZKALLA, S., HASSAN, T. & LUCIER, G. 2009. FRP Shear Transfer Mechanism for Precast, Prestressed Concrete Sandwich Load-Bearing Panels.

SALMON, D. C., EINEA, A., TADROS, M. K. & CULP, T. D. 1997. Full Scale Testing of Precast Concrete Sandwich Panels. *ACI Structural Journal,* 94**,** 354-362.

TOMLINSON, D. G. 2015. *Behaviour of partially composite precast concrete sandwich panels under flexural and axial loads.* PhD, Queen´s University.